Simulation of grating–based X–ray differential phase contrast imaging

Rong Feng[1,2], Liang Ying[1], Yang Yadong[1], Ma Xuehao[1]

(1. School of Electronics and Information Engineering, Tianjin Polytechnic University, Tianjin 300387, China;

2. Tianjin Key Laboratory of Photoelectric Detection Technology and System, Tianjin Polytechnic

University, Tianjin 300387, China)

Abstract: According to the Fresnel diffraction theory, a simulation model of grating–based X–ray differential phase contrast imaging system was established. A PMMA sphere was the image object and the level of X–ray was 30 keV. Through the simulation, the change of the wave front of the X–ray passing through the sphere and phase grating was gotten. In addition, the image of first–order derivative of object phase was extracted by the method of phase –stepping. Furthermore, the influence of Moire fringe contrast on image quality was analyzed. The optimization design of the parameters of the grating was discussed. The simulation results are helpful to optimize the experimental platform, and analyze the factors that affecting the image quality.

Key words: grating–based X–ray differential phase contrast imaging; Fresnel diffraction;

contrast of Moire fringe; phase–stepping

X 射线光栅相衬成像的仿真

荣　锋[1,2],梁　莹[1],杨亚东[1],马雪皓[1]

(1. 天津工业大学 电子与信息工程学院,天津 300387;

2. 天津工业大学 天津市光电检测技术与系统重点实验室, 天津 300387)

摘 要:根据菲涅耳衍射积分理论,提出了 X 射线光栅相衬成像系统的仿真模型。以聚甲基丙烯酸甲酯(PMMA)小球作为成像物体模型,选取 30 keV 的 X 射线做模拟计算。通过仿真,得到了穿过球体和相位光栅的 X 射线波前的变化。采用多步位移法从模拟条纹图中恢复出了 PMMA 小球的相位信息,并分析了莫尔条纹对比度对成像质量的影响,为实际的实验提供可靠的参数选择。经过仿真得到的相移信息与通过实验得到一致,验证了仿真算法的正确性。

关键词:X 射线光栅相衬成像; 菲涅耳衍射; 莫尔条纹对比度; 多步位移

0 Introduction

X–ray absorption imaging technology is an important tool in clinical diagnosis and non–destructive evaluation. However, due to the principle that imaging is based on the absorption difference of materials in X–ray, the image quality of weak absorption materials composed of light elements is quite poor. The interactions of the X–ray with materials can be represented with the complex refractive index, that is the formula $n=1-\alpha+i\beta$, where β is the absorption factor, α is the phase factor, they respectively represent the shift of amplitude and phase after X–ray passing through the object[1]. In the hard X–ray region, the phase factor of object conposed of lighter elements is usually more than 3 orders of magnitude larger than the absorption factor. Therefore, a technique using phase shift to imaging is proposed. Grating–based X–ray differential phase contrast imaging has been viewed as the one of the most potential methods, which is based on the Talbot effect. Placing an analysis grating in the grating self–imaging, the formation of Moire fringes can effectively reduce the requirements of the CCD detector spatial resolution [2]. In 2006, F. Pfeiffer introduced an absorption grating near the X–ray tube to ensure the spatial coherence of the light source, which makes it possible to turn grating–based X–ray differential phase contrast imaging from research into reality[3].

However, there are some problems in grating–based X–ray differential phase contrast imaging system, including complex imaging system and high requirements of imaging condition [4]. Because the source and analysis grating are absorption ones, high Z elements are essential to absorb X–ray. And in order to achieve ideal absorption effect, the aspect ratio of absorption grating is usually ten to one, or even tens to one, which is difficult to achieve in practice[5]. In addition, when the source is a high –energy X –ray, due to the incomplete absorption of the absorption grating, the contrast of the image fringes decreases, causing the image quality deteriorates. Phase stepping method is usually used to extract the phase information during the imaging process, which requires a high accuracy of the stepping platform[6]. Therefore it is vital to put forward a complete set of models about X –ray simulation theory and performance analysis.

Nowadays there are many simulation methods of X–ray phase contrast imaging, including virtual optical simulation method, the scalar diffraction theory [7], the coaxial imaging process of ZEMAX simulation, the light track and coaxial imaging simulation of paraxial scalar diffraction theory. But these methods are all based on the in–line imaging, which is not suitable for grating –based X –ray differential phase contrast imaging system and can't be explained by a unified theory model either. In 2009, Li T T first proposed grating–based X–ray differential phase contrast imaging simulation, but it only focuses on the simulation parameters settings. And there is no analysis of the influence of the experimental conditions on the experimental results[8].

This paper is based on the Fresnel diffraction integral theory, and a PMMA(Polymethylmethacry–late) sphere is used as the image object. We can get the changes of the X –ray wave front passing through the object by simulation. Meanwhile, the Moire fringes formed by grating self–imaging and analysis gratings can be obtained. And the phase shift information contained in the fringes is extracted by the phase stepping method. We extract the first–order derivative of phase distribution of the sphere, which is consistent with the experimental results in related literature. Additionally, by extracting phase information under different contrast conditions, the effect of fringe contrast on image quality is analyzed. Furthermore, some methods of improving the fringe contrast of imaging system are put forward.

1 Imaging system and the principle of phase extraction

The configuration of a typical grating–based X–ray differential phase contrast imaging system is shown in Fig.1. The system is mainly composed of source grating G_0, imaging grating G_1 and analysis grating G_2, with a period of P_0, P_1 and P_2 respectively. And the distance between G_0 and G_1 is l, between G_1 and G_2 is Z_L.
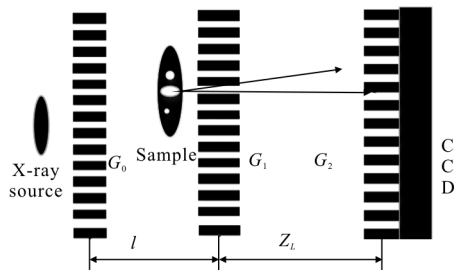

Fig.1 Grating–based X–ray differential phase contrast imaging

When the experimental device meets $P_0/P_2=l/Z_L$, according to the principle of Lau effect, using ordinary X–ray source can meet the grating based phase contrast imaging system requirements[9].

In this system, the function of G_0 grating is to divide the incoherent X–rays emitted by ordinary X–ray sources into a series of X–rays, which are coherent and mutually incoherent with each other. G_1 is an imaging grating forming periodic interference fringes at G_2, G_2 with G_1 imaging produce Moire fringe at the first Talbot distance of G_1, which plays a role of mask.

After X–ray passing through the imaging object, the phase shift of the wave front results in the deflection of the X–ray. So the phase information can be extracted according to the changes of the refraction angle. The refraction angle can be expressed as:

$$\theta=\frac{\lambda}{2\pi}\frac{\partial\Phi}{\partial x}=\frac{\partial\int_{l_0}\alpha(x,y,z)\mathrm{d}z}{\partial x} \tag{1}$$

Where l_0 is the thickness of the imaging sample, λ is the wavelength of X–ray, and Φ is the total phase shift.

X–ray travels from phase grating to analysis grating and produces Moire fringe, in which the phase shift can be calculated using:

$$\phi=\frac{2\pi Z_L}{P_2}\frac{\partial\int_{l_0}\alpha(x,y,z)\mathrm{d}z}{\partial x} \tag{2}$$

In the grating phase contrast imaging, phase stepping method is usually used to extract the phase information of the image objects. Assuming that grating shift step is N, the CCD detector records a light intensity information when the grating moves each time. Hence, the light intensity of number K step is given by:

$$I_K(x,y)=\sum_n b_n(x,y)\exp\left[i2\pi n\left(\frac{K}{N}+\frac{\phi(x,y)}{2\pi}\right)\right]\approx$$
$$b_0(x,y)+b_1(x,y)\exp\left[i2\pi\left(\frac{K}{N}+\frac{\phi(x,y)}{2\pi}\right)\right] \tag{3}$$

Where $b_n(x,y)$ is the Fourier coefficient and n is series. The amount of phase shift can be obtained by combining N equations,

$$\phi(x,y)=\arctan\left[\frac{\sum_{K=1}^{N}I_k(x,y)\sin\left(2\pi\frac{K}{N}\right)}{\sum_{K=1}^{N}I_k(x,y)\cos\left(2\pi\frac{K}{N}\right)}\right]\frac{\partial\int_{l_0}\alpha(x,y,z)\mathrm{d}z}{\partial x} \tag{4}$$

Refraction angle of the image object with respect to the background can be described as:

$$\theta=\frac{P_2[\phi^f-\phi^b]}{2\pi Z_L} \tag{5}$$

Where ϕ^f, ϕ^b represent the phase shift induced by objects and background respectively.

The image quality of grating phase contrast imaging largely depends on the coherence of the light field, and the fringe contrast can directly reflect the coherence[10],

$$V=\frac{I_{\max}-I_{\min}}{I_{\max}+I_{\min}} \tag{6}$$

As can be seen from Eq.(6), the higher the X–ray coherence, V will be close to 1 if $I_{\min}$ is small enough.

2 Simulation model and the optical path simulation procedures

In this part, we mainly introduce the

establishment of simulation model and simulation steps. Firstly, applying the X–ray irradiation. The wave front before specimen is $U_0(x,y)$. Due to the imaging optical path meets Lau effect, X–ray passing through the source grating can be viewed as a line light source that is not coherent with each other. In order to simplify the simulation steps, we use a single line light source to simulate, the overall effect of light intensity can be obtained by using the a single line light intensity multiplied by N (The total number of line source). The wave front after X–ray passing through the image object can be expressed as $U_1(x,y)$. The interaction of the X–ray with the image object can be represented by a complex index of refraction, $n = 1 - \alpha + i\beta$, In order to represent the effect of the image object and X–ray, complex refractive index should be subtracted from the effect of X–ray propagation in vacuum, i.e. the refractive index should be described as $n_1 = n - 1$. The transfer function of sample is $\exp(i \times K \times n_1 \times \text{thickness})$, the wave front is expressed as $U_1(x,y) = U_0(x,y) \times \exp(i \times K \times n_1 \times \text{thickness})$. In order to simplify the simulation steps and reduce the difficulty of simulation, assuming that the sample is placed next to the imaging grating. The wave front behind imaging grating can be expressed as $U_2(x,y)$. The π phase grating is used as imaging grating to improve the light energy utilization and eliminate the background light intensity. Here the duty ratio of the phase grating is 0.5, the transfer function $T(x,y)$ in a half cycle is 1, another is $\exp(i \times \varphi)$, and $U_2(x, y) = U_1(x,y) \times T(x,y)$.

After X–ray through the phase grating and spreads fractional Talbot distance, the wave front turns to $U_3(x,y)$. The fractional Talbot distance $Z_L = P_1^2/8\lambda$, during which the diffraction meets the Fresnel conditions. And the Fresnel diffraction integral expression is given as:

$$U_3(x,y) = \frac{\exp(jkZ_L)}{j\lambda Z_L} \otimes$$

$$\iint U_2(x_0,y_0)\exp\left\{jk\frac{[(x-x_0)^2+(y-y_0)^2]}{2Z_L}\right\}\mathrm{d}x_0\mathrm{d}y_0 \qquad (7)$$

Where $k = 2\pi/\lambda$, however the calculation based on formula (7) is too trouble, which can be simplified in time domain,

$$U_3(x,y) = U_2(x_0,y_0) \otimes \left\{\frac{\exp(jkZ_L)}{j\lambda Z_L}\exp\left[jk\frac{(x^2+y^2)}{2Z_L}\right]\right\} \qquad (8)$$

Considering that a great deal of machine time and memory consumption has to be spent performing the time domain convolution. So we prefer handling the problem in the frequency domain.

$$U_3(x,y) =$$

$$FFT^{-1}\left\{FFT\{U_2(x_0,y_0)\}\exp\left\{jkZ_L\left[1-\frac{\lambda^2}{2}(u^2+v^2)\right]\right\}\right\} \qquad (9)$$

Where u, v represent the corresponding spatial frequency of x, y respectively.

The calculation above is under the parallel light conditions, while the source used in practice is the point light. And the expression of the object and the associated imaging magnify M times correspondingly, here $M = l/(l + Z_L)$. In order to reduce the energy loss of X–ray in practice, Z_L is chosen as the first–order Talbot distance, which is much smaller than 1. And M is approximately equal to 1. Therefore there is almost no difference of the imaging under point or parallel light conditions. And this is the reason why we select the parallel light to simulate in this paper.

The wave front of X–ray passing through the analysis grating is $U_4(x,y)$, the duty ratio of analysis grating is also 0.5, the transfer function $T_1(x,y)$ in a half cycle is 1, another is 0, so $U_4(x,y) = U_3(x,y) \times T_1(x,y)$. According to the steps of the multi–step displacement, we can get the distance of analysis grating. Furthermore, the Moire stripe image can be obtained. The Moire stripe image we get above can be synthesized into a CCD image, since the size of CCD pixels is around ten times of the analysis grating. That is to say, a

CCD pixel contains several Moire stripes. So we should take this into consideration when we talk about CCD image synthesis. According to the synthesized CCD image and formulas (8) and (9), the phase shift information of the imaging object can be obtained. We can also discuss the influence of contrast ratio on image quality by varying the contrast during simulation.

3 Simulation parameters selection and simulation results analysis

The energy of X-ray is set to 30 keV during the simulation, and the wavelengths can be represented by $1.24e^{-9}$/energy. The image object is a PMMA sphere, which is half of the imaging field of view in diameter. The refractive index is $n=1-2.961 \cdot e^{-7}+i \cdot 1.021 \cdot e^{-10}$, the π phase grating with a period of 4 μm, while the analysis grating cycle is 2 μm and the pixel size of CCD detector is 20 μm×20 μm. Due to the CCD pixel size in simulation is one order of magnitude larger than the analysis grating period, the detector image resolution is low.

In order to guarantee the correctness of the simulation, first of all, the Talbot effect simulation is carried out to verify the correctness of the Fresnel diffraction program without imaging object. We can get the light intensity distribution at different distances of π phase grating in Fig.2(a). According to the Talbot effect, we can get $Z_L=nP_1^2/2\lambda\xi^2$. In π phase grating, n is odd and ξ is 2. Imaging cycle is the half of phase grating cycle. It can be seen from Fig.2 (a), both the Talbot distance and the imaging period meet the characteristics of Talbot imaging, which verifies the correctness of the Fresnel diffraction procedure in this paper.

After placing the imaging objects, the distribution of the fringes at the fractional Talbot is Fig.2(b). Due to the refraction of the object, the

stripes are distorted and deflected. And bending appeared a certain regularity: the sphere internal refraction angle shifts slowly and stripes move less. While the edge of refraction angle changes faster and have larger movement. In addition, the edge of the sphere has edge enhancement effect. These features are consistent with the experimental results, which proves the correctness of the loading method of imaging objects in simulation.
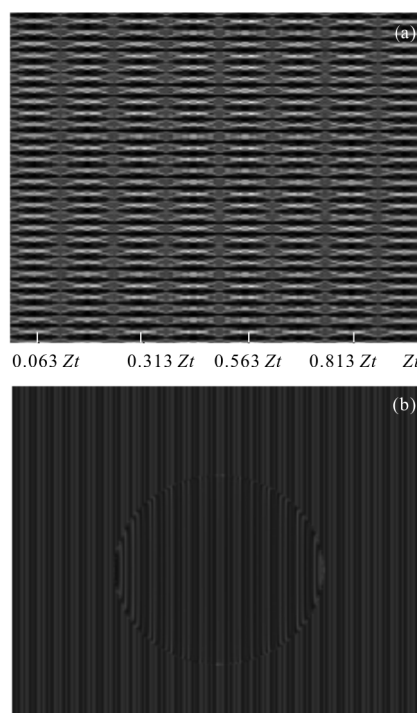

Fig.2 (a)Light intensity distribution at different distances of π phase grating; (b) fringe pattern before analysis grating

According to the above simulation steps, we get the first-order derivative distribution of CCD image phase, as shown in Fig.3(a). While Fig.3(b) is the first-order derivative distribution of the sphere corresponding cross-section in Fig.3 (a). The result shows that the first-order derivative of the phase can correctly reflect the phase shift caused by the refraction of PMMA sphere, which is in agreement with the experimental results and proves that the proposed simulation model is correct.
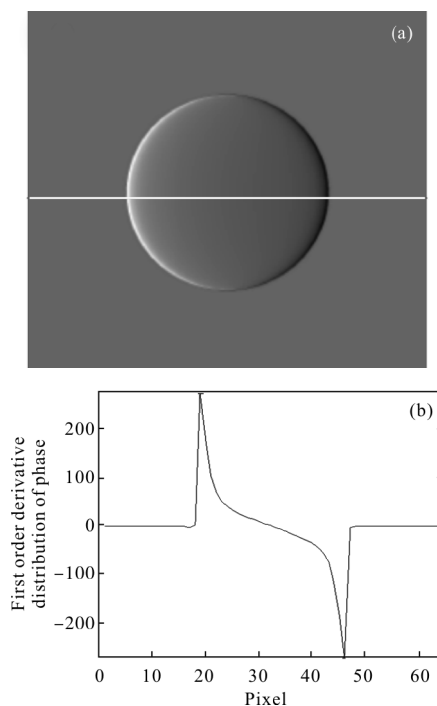
Fig.3 Simulation results, (a) using phase stepping method to extract the first−order derivative of phase distribution; (b) the first−order derivative distribution of the sphere corresponding cross−section(white line) in (a)

The first−order deri vative distribution of sphere center section under different contrast can be obtained by varying the transfer function of analysis grating. As can be seen from Fig.4 (a), when the contrast is 1, 0.8, 0.6, the trend of the first−order derivative of the phase distribution is correct, which reflects the refraction induced by object. While contrast is 1 and 0.8, it has little influence on the quality of X −ray imaging. However, when the contrast reduces to 0.6, the phase shift is decreased obviously. Although refraction angle information still can be extracted from the imaging, the noise is very large and the image quality degrades.

In Fig.4(b), if we set the contrast to 0.3, selecting the center and edge cross−section of the sphere, the first derivative of the phase distribution of different cross sections can be obtained. Comparing the curve marked by a triangle symbol in Fig.4 (a), when the contrast drops to 0.3, the

trend of the whole curve of the central section is different from that of the normal imaging, and the phase shift of information can′t be extracted yet. Comparing the two curves in Fig.4(b), we can find the different effect of X−ray on different regions. Although the contrast of both curves is 0.3, the spherical edge section has a smaller phase shift, and the whole phase shift curve trend is correct, which reveals that the edge of the PMMA sphere has a strong anti−noise ability.
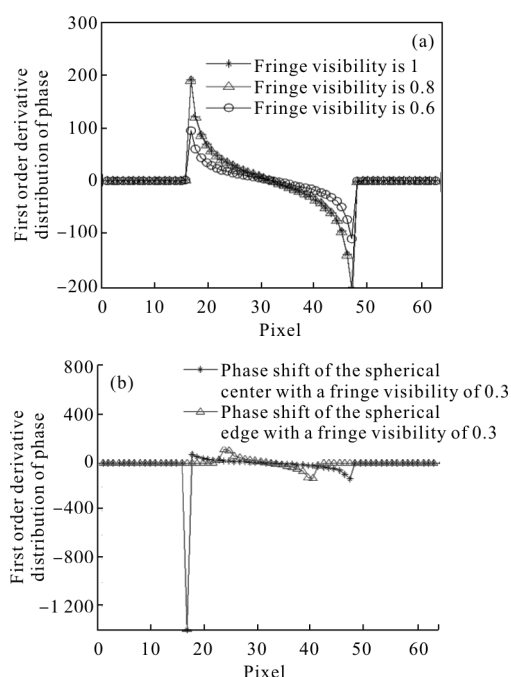

Fig.4 (a) Phase−shift diagrams at different contrasts; (b) phase−shift diagrams with different cross−sections for a contrast of 0.3

As can be seen from Fig.4 (a) and (b), the contrast of the imaging system has an important influence on the extraction of phase information. Therefore, it is necessary to improve the contrast of the imaging system as much as possible. There are some measures to improve contrast, such as selecting the grating with a duty ratio of 0.5 for experiment[11]. When choosing the source grating and the analysis grating, be sure to select high−Z material filling and improve the grating aspect ratio as much as possible. When adjusting the optical path during the experiment, it is important

to ensure the parallelism of the gratings. When selecting CCD detector, the choice of cooling detector can reduce noise best.

4　Conclusion

Based on the Fresnel diffraction and phase stepping method to extract phase information, this paper describes the simulation model of grating –based X –ray differential phase contrast imaging in detail. Furthermore, the phase information of the image object is extracted, and simulation results show that the calculation of simulation optical path is right. Additionally, by extracting phase information under different contrast conditions, the effect of fringe contrast on image quality is analyzed. Meanwhile, some methods of improving the fringe contrast of imaging system are put forward. Grating imaging experiment platform is complex, while simulation model proposed in this paper can quickly test the influence of various parameters on the imaging quality of the imaging system.

References：

[1]　Wang Z, Hauser N, Kubikhuch R A, et al. Quantitative volumetric breast density estimation using phase contrastmammography [J]. *Physics in Medicine and Biology*, 2015, 60(10): 4123–4135.

[2]　Li J P, Chen L, Fang B. Study on diffraction efficiency of phase interferometer for dynamic interferometer [J]. *Infrared and Laser Engineering*, 2015, 44 (9): 2696–2701. (in Chinese)

[3]　Lei Y H, Du Y, Li J, et al. Application of Bi absorption gratings in grating–based X–ray phase contrast imaging [J]. *Applied Physics Express*, 2013, 6(11): 117301.

[4]　Lider V V, Kovalchuk M K. X –ray phase –contrast methods [J]. *Crystall Ography Reports*, 2013, 58 (6): 769–787.

[5]　Munro P R, Hagen C K. A simplified approach to quantitative coded aperture X –ray phase imaging [J]. *Optics Express*, 2013, 21(9): 11187–11201.

[6]　Miao H, Chen H, Bennett E E, et al. Motionless phase stepping in X –ray phase contrast imaging with a compact source [J]. *Proceedings of the National Academy of Sciences of the United States of America*, 2013, 110(48): 19268–19272.

[7]　Li T T, Li H. X –ray differential grating imaging simulation[J]. *System Simulation Express*, 2009, 21(2): 204–210. (in Chinese)

[8]　Mu Y N, Li P, Wang H. Contrastive analysis of single grating and double grating diffraction angle detection [J]. *Infrared and Laser Engineering*, 2014, 43 (5): 1616–1620. (in Chinese)

[9]　Weitkamp T. Phase retrieval and differential phase – contrast imaging with low–brilliance X–ray sources[J]. *Nature Physics*, 2006, 2(4): 258–261.

[10]　Lei Y H, Huang J H. Improvement of visibility of moiré fringe in X –ray differential phase –contrast imaging [J]. *Journal of Shenzhen University Science and Engineering*, 2016, 33(5): 506–510.

[11]　Huang J H, Lin J Y. Analysis and simulation of mid– energy X –ray grating phase contrast microscopy imaging [J]. *Acta Optica Sinica*, 2011, 31 (10): 1034001. (in Chinese)